



Published in final edited form as:

Neuroimage. 2021 December 15; 245: 118682. doi:10.1016/j.neuroimage.2021.118682.

Hippocampal acidity and volume are differentially associated with spatial navigation in older adults

Matthew J. Sodoma^{a,*}, Rachel C. Cole^{b,h}, Taylor J. Sloan^a, Chase M. Hamilton^a, James D. Kent^{b,i}, Vincent A. Magnotta^{c,d,e,f,g}, Michelle W. Voss^{a,b,c}

^aDepartment of Psychological and Brain Sciences, University of Iowa, Iowa City, IA 52242, USA

^bInterdisciplinary Graduate Program in Neuroscience, University of Iowa, Iowa City, IA 52242, USA

^cIowa Neuroscience Institute, University of Iowa, Iowa City, IA 52242, USA

^dDepartment of Radiology, University of Iowa, Iowa City, IA 52242, UCA

^eDepartment of Biomedical Engineering, University of Iowa, Iowa City, IA 52242, USA

^fDepartment of Psychiatry, University of Iowa, Iowa City, IA 52242, USA

^gPappajohn Biomedical Institute, University of Iowa, Iowa City, IA 52242, USA

^hDepartment of Neurology, University of Iowa, Iowa City, IA, 52242, USA

ⁱDepartment of Psychology, University of Texas at Austin, Austin, TX, 78712 USA

Abstract

The hippocampus is negatively affected by aging and is critical for spatial navigation. While there is evidence that wayfinding navigation tasks are especially sensitive to preclinical hippocampal deterioration, these studies have primarily used volumetric hippocampal imaging without considering microstructural properties or anatomical variation within the hippocampus. T1 ρ is an MRI measure sensitive to regional pH, with longer relaxation rates reflecting acidosis as a marker of metabolic dysfunction and neuropathological burden. For the first time, we investigate how measures of wayfinding including landmark location learning and delayed memory in cognitively normal older adults ($N = 84$) relate to both hippocampal volume and T1 ρ in the anterior and posterior hippocampus. Regression analyses revealed hippocampal volume was bilaterally related to learning, while right lateralized T1 ρ was related to delayed landmark location

This is an open access article under the CC BY-NC-ND license (<http://creativecommons.org/licenses/by-nc-nd/4.0/>)

*Corresponding author. matthew-sodoma@uiowa.edu (M.J. Sodoma).

Credit authorship contribution statement

Matthew J. Sodoma: Conceptualization, Methodology, Validation, Formal analysis, Investigation, Data curation, Writing – original draft, Writing – review & editing, Visualization. **Rachel C. Cole:** Methodology, Validation, Investigation, Data curation, Writing – review & editing. **Taylor J. Sloan:** Methodology, Validation, Investigation, Data curation, Writing – review & editing. **Chase M. Hamilton:** Investigation, Data curation, Writing – review & editing, Project administration. **James D. Kent:** Software, Methodology, Validation, Writing – review & editing. **Vincent A. Magnotta:** Software, Methodology, Resources, Writing – review & editing, Funding acquisition. **Michelle W. Voss:** Conceptualization, Resources, Writing – original draft, Writing – review & editing, Supervision, Project administration, Funding acquisition.

Supplementary materials

Supplementary material associated with this article can be found, in the online version, at doi:10.1016/j.neuroimage.2021.118682.

memory and bilateral T1 ρ was related to the delayed use of a cognitive map. Overall, results suggest hippocampal volume and T1 ρ relaxation rate tap into distinct mechanisms involved in preclinical cognitive decline as assessed by wayfinding navigation, and laterality influenced these relationships more than the anterior-posterior longitudinal axis of the hippocampus.

Keywords

Spatial navigation; Cognitive aging; Hippocampal t1 ρ ; Hippocampal volume; Longitudinal axis

1. Introduction

Spatial navigation skills deteriorate in aging. This decline in skill is one clue that the impact of aging on the brain is beginning to take its course. In aging, poor navigational skills can affect functional independence and quality of life. Poor navigation skills are associated with hippocampal volume atrophy and biomarkers of neurodegeneration that track with mild cognitive impairment (MCI) and risk for Alzheimer's Disease (AD) (Allison et al., 2016, 2019; Head and Isom, 2010; Levine et al., 2020). However, given the subtlety of preclinical hippocampal deterioration, there is a need for specifying hippocampal mechanisms associated with a decline in spatial navigation. Here, we use approaches that take advantage of new evidence from cognitive neuroscience and biomarkers of brain aging to detect spatial navigation decline.

1.1. Hippocampal aging

The hippocampus is known to change across the lifespan, both as part of a normal lifespan trajectory and in response to both beneficial and detrimental lifestyle factors. On average, hippocampal atrophy remains relatively mild until the late 50s, after which there is accelerated shrinkage, resulting in a non-linear atrophy pattern across the lifespan (Fjell et al., 2013; Raz et al., 2005). Hippocampal deterioration is relevant for understanding performance decline in episodic memory, a form of memory needed to bind elements of our experiences over space and time. Episodic memory has been shown to decline with age-related hippocampal atrophy (Gorbach et al., 2017; Head et al., 2009). While these studies generally support the role of hippocampal shrinkage in age-related episodic memory decline, the hippocampus has often been treated as a homogenous structure. Some studies have characterized age-related hippocampal atrophy according to subfields and there is some promising evidence that CA1 shows the most robust volumetric decline with age (de Flores et al., 2015). However, findings from a subfield-based model have been mixed overall, in part due to lack of standardized processes for imaging acquisition and subfield parcellation (Carr et al., 2017; de Flores et al., 2015; Foster et al., 2019). Further, segmentation of the hippocampus into subfields typically comes at the cost of distinctions across the anterior-posterior hippocampus and cannot be examined without ultra-fine spatial resolution.

Although the hippocampus has commonly been treated as a homogenous structure to understand its role in age-related memory decline, and with mixed results regarding subfields, more recent evidence suggests the hippocampus is affected differently by age across the anterior-posterior longitudinal axis. Langnes et al. (2020) completed a

longitudinal study containing 1790 individuals across the lifespan with an average of 2.7 years of follow-up and showed that the posterior hippocampus was more affected by advanced age-related atrophy than the anterior. Evidence from cognitive neuroscience approaches suggests these differences in age-related shrinkage along the anterior-posterior axis are relevant for understanding age-related episodic memory decline. Poppenk & Moscovitch (2011) showed from 4 different studies that posterior hippocampal volume was most strongly associated with post-encoding and retrieval processes. Similarly, two meta-analyses spanning PET and MR functional imaging methods found the posterior hippocampus to be most strongly associated with retrieval, whereas the anterior hippocampus was more strongly linked to encoding (Lepage et al., 1998; Spaniol et al., 2009).

1.2. Spatial navigation

The hippocampus is an important piece to many different cognitive processes that are mostly studied in isolation. For instance, the hippocampus supports episodic memory, our ability to recall facts and events related to our experiences. A separate line of research has shown the hippocampus supports spatial navigation, our ability to calculate and navigate our environments through space and time. Bringing episodic memory and spatial navigation lines of research together, relational memory theory conceptualizes relational binding as a core process supported by the hippocampus to explain the central role of the hippocampus in episodic memory and spatial navigation. From this view, spatial and temporal features of the environment are necessarily encoded in a relational form to guide the formation and retrieval of memories for personal episodes and navigation through our environments (Eichenbaum and Cohen, 2014).

Similar to the importance of the anterior-posterior hippocampus for episodic memory, data across lesion studies, functional imaging, and volumetric imaging support that cognitive processes critical for spatial navigation rely on different segmentations of the hippocampus concerning laterality and the anterior-posterior axis (see reviews Grady and Ryan, 2017; Poppenk et al., 2013). Data from rodent studies, at the microscale, link the posterior hippocampus with spatial processing more so than the anterior, supported by observations for anterior-posterior gradients in the elements of spatial memory representations like grid cells and place cells, as well as dissociations implicating the posterior (but not the anterior) hippocampus in spatial processing during the Morris water maze (Burwell, 2004; Jung et al., 1994; Moser et al., 2008; Moser and Moser, 1999). In human cognitive neuroscience, at the macroscale, studies ranging from volumetric to functional MRI have also consistently identified posterior hippocampal and medial temporal regions as involved in spatial navigation (Bohbot et al., 2007; Grön et al., 2000; Hartley and Harlow, 2012; Iaria et al., 2003, 2007; Maguire et al., 2000, 2006; Maguire, Woollett, 2006; Sherrill et al., 2013; Wegman et al., 2014; Wolbers and Büchel, 2005; Woollett and Maguire, 2011), with some evidence suggesting right lateralization (Konishi and Bohbot, 2013; Maguire et al., 1998; Nedelska et al., 2012; Smith and Milner, 1981; Wegman et al., 2014). Across both micro and macroscales, these studies generally support a preferential role of the right posterior hippocampus in wayfinding through the formation and use of cognitive maps, which are conceptualized as a birds-eye memory representation for the environment (Tolman,

1948). Classic examples of hippocampal plasticity with the persistent formation and use of cognitive maps come from studies reporting greater gray matter in the right posterior hippocampus of London taxi and bus drivers (Maguire et al., 2000; Maguire, Woollett, 2006; Woollett and Maguire, 2011). Given this evidence, while the hippocampus atrophies with aging, we would expect right posterior hippocampal atrophy to affect navigation that depends on forming or using cognitive maps more so than atrophy of the anterior hippocampus.

To test this idea, in the current study older adults completed a virtual wayfinding task designed to measure cognitive map learning and retrieval. This task has been shown to be related to bilateral hippocampal volume in older adults, related to CSF biomarkers that are associated with preclinical AD, and predictive of subsequent cognitive decline and development of AD (Allison et al., 2016, 2019; Head and Isom, 2010; Levine et al., 2020). Specifically, the task is derived from Head & Isom (2010), with additional learning test trials adapted from Allison et al. (2016) to assess cognitive map learning. This modified task has two phases: a learning phase and a 30-minute delayed phase. The learning phase elicits the formation of a cognitive map by having participants navigate a virtual environment to learn the location of objects (Fig. 1A). Object-location binding is tested across four learning trials that assess memory for object locations when the virtual world is viewed from a top-down survey perspective (landmark location identification) (Fig. 1B). The use of a cognitive map is tested in a delayed phase by requiring participants to find objects in the virtual world when placed at different starting locations and navigating from a first-person perspective (delayed wayfinding test). Lastly, in the delayed phase, cognitive map retrieval is tested with another top-down survey perspective object location test (delayed landmark location identification). Across the four studies using variants of this task, bilateral hippocampal volume has been associated with cognitive map formation in one study (Levine et al., 2020) total distance traveled and latency in cognitive map usage in another study (Head and Isom, 2010), and not tested in the other two studies (Allison et al., 2016, 2019).

1.3. T1 ρ imaging

T1 ρ is a non-invasive MRI measure that is sensitive to regional pH, with longer relaxation rates reflecting acidosis as a marker of metabolic dysfunction and neuropathological burden. Although not well-known in the preclinical aging field, T1 ρ is not a new technique, having first been described in 1955 (Redfield, 1955), applied to MRI in 1985 (Sepponen et al., 1985), and used in the body to distinguish damaged tissue based on cellular pathologies affecting acidity (see review, Wáng et al., 2015). More recently in the last decade, T1 ρ has been measured in the brain and shown to have longer relaxation rates within brain regions distinctly affected by pathologies in AD (Haris et al., 2009, 2015; Haris et al., 2011, 2011), Parkinson's disease (Nestrasil et al., 2010), Bipolar disorder (Johnson et al., 2015), and Huntington's disease (Wassef et al., 2015) among patients affected by each of these neurodegenerative conditions. Further, T1 ρ is a non-invasive measure of tissue pH, shown in phantoms, mouse models, and human samples (Heo et al., 2014; Kettunen et al., 2002; Magnotta et al., 2012; Owusu et al., 2020). Increases in acidity are known to occur in diseased tissues, inflammation, aging, and neurodegenerative disease, thus we would expect T1 ρ to be related to cognitive outcomes related to aging. Most relevant to the

current study, (Boles Ponto et al., 2020) compared T1 ρ imaging, [11C]PiB PET imaging, and fluorodeoxyglucose PET imaging, and found that longer T1 ρ was associated with age, higher amyloid burden, abnormal cerebral glucose metabolism, Trail Making B-A and Logical memory. However, no studies have tested whether hippocampal T1 ρ is sensitive to the subtle wayfinding difficulties in cognitively normal older adults nor compared T1 ρ to hippocampal volume.

1.4. Current study

The goal of this study was to assess whether hippocampal volume and T1 ρ tap into similar or distinct mechanisms involved in preclinical memory decline as assessed by wayfinding navigation and the extent to which these relationships are regionally specific along the anterior-posterior longitudinal axis of the hippocampus. We predicted that smaller right posterior hippocampus and longer T1 ρ in the right posterior hippocampus would be detrimental to performance across all task conditions including landmark location learning, delayed retrieval, and wayfinding. We expected the posterior hippocampus to be most predictive of performance at the delay phase, due to its involvement in both episodic retrieval and spatial memory processes. Given the sensitivity of cognitive map learning to biomarker positive status among cognitively normal individuals (Allison et al., 2016) and the presumed sensitivity of T1 ρ to subtle pathology, we further predicted individuals with longer T1 ρ and smaller posterior hippocampal volume would be the most impaired on cognitive map learning.

2. Methods

All imaging and behavioral data were collected at the University of Iowa in Iowa City, IA. Participants were recruited from the surrounding area with flyers, posters, emails, and informational stands at local events. All participants provided consent to the study procedures approved by the University of Iowa Institutional Review Board (IRB). Data were collected as part of two parent studies with common measures of T1 and T1 ρ imaging and spatial navigation.

2.1. Participants

For Study 1, data were collected from 40 community-dwelling healthy older adults (see Table 1 for demographics). Eligible participants met the following criteria: (1) between ages of 50 and 80 years old, (2) free from psychiatric and neurological illness and no history of stroke or chronic metabolic diseases, (3) no history of brain trauma or brain surgery, (4) no self-reported regular use of medications affecting the central nervous system (psychotropics, chemotherapy, etc.), (5) >24 on MMSE-2, (6) able to complete an MRI scan (i.e. no implants above the waist, can comfortably fit in scanner, etc.), (7) corrected vision of 20/40, (8) able to complete a sub-maximal aerobic fitness test, (9) do not require caregiver assistance, and (10) not colorblind. Following data collection, four subjects were excluded due to artifacts in the T1 ρ image, leaving $N=36$ subjects eligible for inclusion in the pooled analysis.

Data from Study 2 were collected at the baseline assessment of a randomized control trial exercise intervention (NCT03114150). The first half of enrolled participants with a baseline MRI on the same scanner model were considered eligible for analyses ($N=50$) (see Table 1 for demographics). Eligible participants met the following criteria: (1) were between ages of 55 and 80 years old, (2) free from psychiatric and neurological illness and no history of stroke or chronic metabolic diseases, (3) no history of brain trauma or brain surgery, (4) no self-reported regular use of medications affecting the central nervous system (psychotropics, chemotherapy, etc.), (5) >20 on MoCA, (6) able to complete an MRI scan (i.e. no implants above the waist, can comfortably fit in scanner, etc.), (7) corrected vision of 20/40, (8) able to complete a supervised maximal graded exercise test, (9) do not require caregiver assistance, and (10) not colorblind. Following data collection, two subjects were removed due to artifacts in the $T1\rho$ image, leaving $N=48$ subjects eligible for inclusion in the pooled analysis.

Participants did not differ significantly in their age, proportion female, or years of education (see Table 1). With the consistencies in age, biological sex, years of education, using similar $T1$ and $T1\rho$ sequences on the same scanner, and generally similar exclusion criteria, we collapsed across each study to have a larger pool of participants to support more complex statistical analysis. Previous cross-sectional studies using this spatial navigation task included 47 participants (Head and Isom, 2010), 69 participants (Allison et al., 2016), and 30 participants (Allison et al., 2019) with either a larger age spectrum (young vs old) or a cognitive spectrum (Normal, MCI, AD) and simpler models using bilateral hippocampi or single CSF biomarker. Therefore, given that our effect size was relatively unknown and our sample homogenous across age and cognitive spectrums, we chose to collapse across the two samples to increase power (see supplementary data for post-hoc power analysis).

2.2. MRI acquisition

All MRI data were collected with a 3.0T General Electric (GE) Discovery MR750w MRI Scanner using a 32-channel head coil at the University of Iowa Magnetic Resonance Research Facility. For Study 1, high-resolution anatomical images were collected via a three-dimensional fast spoiled gradient echo sequence (FSPGR) BRAVO $T1$ scan with the following parameters: $TI=450$ ms, $TE=3.248$ ms, $TR=8.464$ ms, flip angle= 12° , Acquisition Matrix= $256 \times 256 \times 176$, $FOV=256 \times 256 \times 176$, 1 mm X 1 mm X 1 mm voxels. Three-dimensional $T1\rho$ images were acquired using a 3D CUBE sequence with the following parameters: $TE=29.6$ ms, $TR=3000$ ms, $FOV=256 \times 256 \times 208$, Acquisition Matrix= $128 \times 128 \times 104$, Bandwidth= 488 Hz/pixel, spin-lock frequency= 500 Hz, spin-lock times= 10 ms, 50 ms, 2 mm X 2 mm X 2 mm voxels.

For Study 2, high resolution anatomical images were collected via a three-dimensional fast spoiled gradient echo sequence (FSPGR) BRAVO $T1$ scan with the following parameters: $TI=900$ ms, $TE=3.168$ ms, $TR=8.388$ ms, flip angle= 8° , Acquisition Matrix= $256 \times 256 \times 196$, $FOV=256 \times 256 \times 196$, 1 mm X 1 mm X 1 mm voxels. Three-dimensional $T1\rho$ images were acquired using a 3D CUBE sequence with the following parameters: $TE=28.89$ ms, $TR=3002$ ms, $FOV=256 \times 256 \times 208$, Acquisition Matrix= $128 \times 128 \times 104$, Bandwidth= 488

Hz/pixel, spin-lock frequency=500 Hz, spin-lock times=10 ms, 50 ms, 2 mm X 2 mm X 2 mm voxels.

For both studies, other magnetic resonance imaging scans were collected within the same imaging session but are not described as they are beyond the scope of the current report.

2.3. MRI analysis

T1w images were preprocessed using fmriprep (version 1.2.1). Hippocampal masks and volume data were then extracted from automated Freesurfer (version 6.0) segmentations for each participant. For hippocampal anterior-posterior segmentations, the Freesurfer left and right hippocampal masks were transformed to the MNI152 template. Left and right hippocampal masks were further split into anterior-posterior subregions by splitting at $y = -21$ for each hemisphere independently, in the MNI resampled brain as suggested by (Poppenk et al., 2013) and recently applied in Langnes et al. (2020). Voxels anterior to this point were considered anterior hippocampus, while voxels posterior to this point were considered posterior hippocampus. The subsequent masks were then transformed to subject-specific space, and the intersection of the Freesurfer hippocampal segmentation mask and the anterior-posterior masks were the resulting hippocampal segmentations from which anterior and posterior volume were determined. Each hippocampal segmentation was adjusted for intracranial volume (ICV).

To isolate brain tissue, a multi-algorithm approach created a probabilistic map of skull-stripped brain masks using algorithms of AFNI's 3dSkullStrip, FSL's Brain Extraction Tool, FreeSurfer's mri_watershed, and the Marker Based Watershed Scalper (for script information see <https://github.com/jdkent/MBA>). Brain-masked T1 weighted images were segmented with FSL's FAST algorithm into gray matter, white matter, and CSF. The resulting masks were used to remove the ventricle and extracerebral CSF from the T1 ρ maps. T1 ρ relaxation times were calculated using a mono-exponential signal decay model by fitting voxel intensities versus the spin-lock times at 10 ms and 50 ms. Each T1 ρ image was corrected for N4 inhomogeneity using the Advanced Normalization Tools (ANTs) N4BiasFieldCorrection and then each T1 ρ image was co-registered with the T1-weighted anatomical images via an in-house modification of the open-source Advanced Neuroimaging Tools (ANTs) script (antsRegistration_SyN). Each T1 ρ image was acquired separately and then co-registered before calculation of the T1 ρ relaxation times which helps to reduce motion related artifacts. To help protect against CSF influencing the T1 ρ values, T1 ρ maps were threshold at intensities between 5 ms and 150 ms. Using the above anterior-posterior hippocampal masks for hippocampal volume, median T1 ρ values were extracted from each of the hippocampal segmentation masks. T1 weighted anatomical and T1 ρ maps were visually inspected for artifacts by two raters (MS) and (VM). Six subjects (4 for Study 1, 2 for Study 2) were removed due to anterior temporal lobe dropout artifacts in T1 ρ signal within regions of interest. For further confirmation of valid and generalizable T1 ρ values, we extracted hippocampal and median temporal lobe (MTL) values from past publications to show our values are within the published range for cognitively normal older adults (see supplementary data). For information related to T1 ρ SNR for different encodings and T1 ρ

error analyses related to our acquisition parameters see publications (Johnson et al., 2020, 2015).

2.3.1. Thalamus as a subcortical comparison region—The thalamus was selected as a comparison region due to its similarities to the hippocampus relative to other subcortical structures. For T1 ρ , we wanted a structure with similar proximity to the head coil, ruling out cortical regions. As compared to other subcortical structures, both the hippocampus and thalamus show significant age-related atrophy for volume, albeit different patterns across the lifespan (Fjell et al., 2013). Within our supplementary data, the SNR for T1 ρ in the thalamus is more similar to the hippocampus than the caudate nucleus, and the hippocampus and thalamus have more similar gray matter/white matter composition. Steps for computing thalamus volume and T1 ρ were the same as the hippocampal masks, with the exception of the anterior-posterior segmentation.

2.4. Behavioral data

The same spatial navigation task was used in parent Studies 1 and 2 (Fig. 1A,B). The task was adapted from Head & Isom (2010), Allison et al. (2016), Allison et al. (2019), and Levine et al. (2020). As a part of larger studies, in both parent Studies 1 and 2, participants completed a battery of cognitive tasks beyond the scope of this report.

2.4.1. Spatial navigation pre-testing—WorldViz Vizard and Autodesk 3ds Max software were used to create a virtual maze environment. In the spatial navigation wayfinding task, participants first familiarized themselves with the joystick by maneuvering a maze containing no objects. To establish their visuomotor capacities, participants were required to navigate to the end of a winding hallway within the 60s-time limit. In our sample of healthy older adults, after joystick practice, all participants were able to complete the test within the allotted time.

2.4.2. Landmark location learning—In the learning phase, each of the 4 learning trials consisted of 5 min of freely navigating the maze from the same starting location while learning where objects were located. Before each trial, participants were instructed to pay attention to the objects and their locations. During the trial, the experimenter provided prompts if parts of the environment were not being explored, but only if necessary. After each learning trial, the participants were given a blank 2-D map of the maze with the starting location identified. Participants were asked to mark each object's location that they could remember with an X. In each trial, the 20 objects remained in the same location in the maze. Participants received a score of 0–20 on each trial for correctly marked objects; accuracy was defined as drawing the center of the X's within a bounding box, which was drawn proportional to the object size (Fig. 1B,C).

For statistical analysis, a linear model was fit to each individual's performance across learning trials. This resulted in subject-specific estimates for trial 1 (intercept) and learning rate (slope) (Fig. 1D). Preliminary analyses showed individual differences followed the same trends for intercept and slope. To limit multiple comparisons derived from having

independent models for each learning trial, landmark location learning is operationalized by subject-specific intercepts.

2.4.3. Delayed wayfinding test—In the delay phase, after an approximately 30-minute delay in which participants completed other cognitive tasks, participants were brought back to the maze environment for the delayed wayfinding test. On each of the 12 trials, participants were given a different object to locate. They were asked to navigate as directly as possible to each object from one of 6 different starting locations. The order of starting positions was the same across participants, and the starting location-object pairings were the same within maze and across participants. Time to complete a given trial was not limited and thus, there were some extreme outliers, where participants continued wandering the maze until the object was found. The distance traveled to each object was winsorized on a trial basis to constrain the influence of trial outliers to the 97.5th percentile. Overall, out of 1056 trials, only 27 trials were winsorized (2.55% of trials across participants). Winsorized trials were not overly concentrated within any one participant: 16 subjects had 1 trial winsorized, 4 subjects had 2 trials winsorized, and 1 subject had 3 trials winsorized. After winsorizing trials, the average distance traveled for the 12 objects was used as the outcome measure.

2.4.4. Delayed landmark location test—After delayed wayfinding test, participants repeated a similar trial to landmark location learning. They were given the same 2-D representation of the maze as before and asked to draw X's where they remembered objects were located. They received a score of 0–20 for correctly marked objects; accuracy was again defined as drawing the center of the X's within a bounding box, which was drawn proportional to the object size.

2.4.5. Controlling for item exposure—While participants explored the maze, the experimenter marked off on a paper checklist for each object the participant encountered. The object was coded dichotomously, either object encountered or not encountered. The number of objects encountered per trial (maximum 20) was summed per trial and we performed simple regressions predicting performance from this exposure variable. As would be expected, item exposure predicted performance and we performed a 2-step regression to control for the influence of item exposure on performance. For landmark location learning, trial 1 item exposure was the predictor and for landmark location magnitude, delayed wayfinding test, and delayed landmark location, the average trial exposure across the four learning trials was the predictor. All subsequent models contain the residuals after controlling for item exposure.

2.5. Statistical analysis

All statistical analysis was completed using R (version 4.0.2) with package lme4 (version 1.1–23) and lmerTest (3.1–2). Data are presented using ggplot2 (version 3.3.2), corrplot (version 0.84), and jtools (version 2.1.1).

To evaluate our hypothesis of regional specificity within the hippocampus, and to avoid having independent models for each hippocampal subregion, separate factor variables were created for subregion (anterior, posterior) and laterality (left, right) to enter in each

regression as independent variables. Adding these factors reduces the number of models needed to analyze the data and avoids needing to apply a correction of multiple comparisons for each of the 4 hippocampal segmentations. Since the same models were applied for T1 ρ and hippocampal volume imaging measures, we applied an MR image domain specific multiple comparison correction with a significance cut-off of $p=.025$.

The relationship between performance variables, volume, and median T1 ρ was tested with six separate linear mixed models fit by maximum likelihood, with each model including factors for subregion, laterality, and covariates (age, sex). We began with the most complex model that would test our hypotheses with subject specific intercepts and slopes. We proceeded through the model simplification procedure starting with the maximal model and removing non-significant interaction terms by comparison of χ^2 (Meteyard and Davies, 2020). Through several steps, we removed the by-subject random slopes for subregion and laterality, and the simplified model included fixed effects of age, sex, years of education, subregion, and laterality with a subregion*laterality interaction term, and random intercepts by subject (see supplementary data for model simplification procedure). This base model stayed consistent for all models investigating spatial navigation performance with imaging measure or spatial navigation outcome measure interchanged. To test whether the relationship of volume or T1 ρ with performance interacted with subregion and laterality, these models included interaction terms for performance* subregion*laterality with either volume or T1 ρ as the dependent variable (see supplementary data for model examples). Factor variables were effect-coded and all variables were Z-score standardized to aid in the interpretation of main effects and 2-way interactions and produce standardized regression coefficients. The thalamus control region analyses used the same models as the hippocampus without the subregion factor.

To understand if T1 ρ and hippocampal volume relationships with spatial navigation performance showed similar patterns to a clinical measure, we ran a supplemental analysis for standardized scores on the MMSE/MOCA using the same models as above (see supplementary data).

3. Results

The results describe three main analyses. First, to inform subsequent models, we ran a correlational analysis between hippocampal subregions, imaging measures, and covariates of age and years of education. Second, for comparison of relationships between imaging measures and age, we examined hippocampal volume and T1 ρ with age with interactions by anterior-posterior subregion and left-right laterality. Third, to understand subregion relationships with spatial navigation, we controlled for age and added interactions with spatial navigation outcomes by subregion and laterality, and interchanged T1 ρ and hippocampal volume as dependent variables in parallel models.

3.1. Hippocampal volume and T1 ρ are not correlated with each other

As shown in Fig. 2B, left and right hippocampal volumes were positively correlated within anterior and posterior subregions and across hemisphere (all r-values > 0.34). In contrast, left and right hippocampal T1 ρ differed in their correlation direction within

anterior-posterior subregions, where the posterior subregions were negatively correlated (posterior, $r(82)=-0.24$, $p=.03$) and the anterior subregions were positively correlated (anterior, $r(82)=0.28$, $p=.009$). Within each hemisphere, anterior and posterior T1 ρ were positively correlated (left, $r(82)=0.68$, $p<.001$; right, $r(82)=0.69$, $p<.001$). Age was negatively correlated with volume in the left anterior ($r(82)=-0.28$, $p=.01$), left posterior ($r(82)=-0.22$, $p=.04$), and right anterior ($r(82)=-0.24$, $p=.03$) subregions but not the right posterior ($r(82)=-0.11$, $p=.32$), whereas age was not significantly correlated with T1 ρ in any subregion (left anterior: $r(82)=-0.1$, $p=.47$, left posterior: $r(82)=0.01$, $p=.11$, right anterior: $r(82)=-0.05$, $p=.15$, right posterior: $r(82)=0$, $p=.20$). Based on the bivariate relationships and model simplification procedure described in 2.5, age and sex were included as covariates in subsequent models. These correlational analyses give the first clue that hippocampal volume and T1 ρ are measuring distinct aspects of hippocampal health. Whereas hippocampal volume was related across hemisphere within L-R anterior, and L-R posterior segmentations, T1 ρ showed the opposite pattern as anterior-posterior subregions were positively correlated within hemisphere (A-P left and A-P right) but differed in correlation direction across hemisphere (L-R anterior positive, L-R posterior negative). Descriptive statistics for volume and T1 ρ for all segmentations and spatial navigation task performance can be found in Table 2.

3.2. Age is related to bilateral hippocampal volume but only right hippocampal T1 ρ

For hippocampal volume, age was a significant predictor across subregions ($\beta = -0.22$, $t(81) = -2.45$, $p = .02$), but there were no interactions with age across subregion and laterality factors (laterality: $\beta = 0.07$, $t(246) = 0.91$, $p = .36$, subregion: $\beta = 0.09$, $t(246) = 1.17$, $p = .24$, see Fig. 3A). Sex was not a significant predictor ($\beta = -0.01$, $t(81) = -0.08$, $p = .93$), such that older participants have smaller bilateral hippocampi independent of sex.

For T1 ρ , age and sex were both significant predictors such that females had longer hippocampal T1 ρ than males ($\beta = .37$, $t(80) = 2.48$, $p = .02$) and there was a significant laterality interaction with age ($\beta = .28$, $t(246) = 2.95$, $p = .004$, see Fig. 3B), but not a significant subregion interaction with age ($\beta = -.05$, $t(246) = -0.61$, $p = .55$). Follow-up analysis revealed that age was predictive of longer T1 ρ in the right hippocampus ($\beta = .25$, $t(80) = 2.40$, $p = .02$), but not left ($\beta = -.10$, $t(82) = -0.91$, $p = .37$).

For the thalamus, age was a significant predictor for volume ($\beta = -.27$, $t(82) = -2.61$, $p = .01$) but not T1 ρ ($\beta = .22$, $t(82) = 2.07$, $p = .04$).

3.3. Hippocampal volume is associated with cognitive map formation

Bilateral hippocampal volume was positively related to landmark location learning, such that those with larger hippocampi formed better initial cognitive maps ($\beta = .19$, $t(80) = 2.34$, $p = .02$, see Fig. 4A and Table 3 for statistics) but there were no interactions with factors of laterality or subregion (laterality: $\beta = 0.07$, $t(246) = 0.86$, $p = .39$, subregion: $\beta = 0.14$, $t(246) = 1.82$, $p = .07$), suggesting there were not differences among subregions related to cognitive map formation. Hippocampal volume was not related to delayed wayfinding test ($\beta = -.001$, $t(80) = -0.02$, $p = .98$, laterality: $\beta = 0.01$, $t(246) = -0.18$, $p = .86$, subregion: $\beta = -0.15$, $t(246) = -1.84$, $p = .07$, see Fig. 4B for models and Table 3 for statistics) or delayed

landmark location ($\beta = .09$, $t(80) = 1.09$, $p = .28$, laterality: $\beta = 0.04$, $t(246) = 0.46$, $p = .65$, subregion: $\beta = 0.12$, $t(246) = 1.46$, $p = .15$, see Fig. 4C for models and Table 3 for statistics). For all models, age was a significant covariate (see supplementary data for simple models of age predicting spatial navigation performance across the 3 spatial navigation tests).

For the thalamus control region, no main effects or interactions with spatial navigation met the $p = .025$ criterion for thalamus volume (see supplementary data).

3.4. Right hippocampal T1 ρ is associated with cognitive map retrieval and bilateral hippocampal T1 ρ is associated with cognitive map usage

T1 ρ was not related to landmark location learning ($\beta = -.05$, $t(80) = -0.69$, $p = .49$, laterality: $\beta = -0.17$, $t(246) = -1.77$, $p = .08$, subregion: $\beta = 0.08$, $t(246) = 0.87$, $p = .38$, see Fig. 4D and Table 3) but was related to delayed measures. For delayed wayfinding test, bilateral T1 ρ was positively related to performance ($\beta = .20$, $t(80) = 2.77$, $p = .007$, see Fig. 4E and Table 3), such that participants with longer T1 ρ across subregions had poorer cognitive map usage and traveled more distance to find objects in the maze. There were no significant interactions with subregion or laterality (laterality: $\beta = 0.06$, $t(246) = 0.63$, $p = .53$, subregion: $\beta = -0.1$, $t(246) = -1.09$, $p = .27$). Yet, for delayed landmark location memory there was a laterality interaction such that longer T1 ρ in only the right hemisphere was related to poorer cognitive map retrieval (laterality: $\beta = -0.23$, $t(246) = -2.48$, $p = .01$, subregion: $\beta = 0.12$, $t(246) = 1.32$, $p = .19$, see Fig. 4F and Table 3).

For the thalamus control region, no main effects or interactions with spatial navigation met the $p = .025$ criterion for T1 ρ .

Overall, the results from 3.3 to 3.4 suggest bilateral hippocampal volume was more related to cognitive map formation than cognitive map retrieval or usage, whereas T1 ρ was more predictive for cognitive map retrieval and usage in the delayed phase: delayed landmark location memory (right lateralized) and delayed wayfinding test (bilateral).

3.4.1. Right lateralized T1 ρ relation to landmark location is not unique to the consolidation period and is present at the end of the learning phase—

As a follow-up analysis, to understand if T1 ρ was preferentially related to the consolidation period associated with delayed performance rather than performance present at the end of the learning phase, we examined the landmark location magnitude, quantified as performance on the fourth learning trial. Similar to the results for delayed landmark location memory, there was a laterality interaction (laterality: $\beta = -0.29$, $t(246) = -2.84$, $p = .005$, subregion: $\beta = 0.06$, $t(246) = 0.64$, $p = .52$), such that lower landmark location magnitude was related to longer T1 ρ in the right hemisphere, but not left. Additionally, landmark location learning magnitude and delayed landmark location memory were positively correlated ($r = 0.80$, $p < .001$, see supplementary data for all correlations between task phases). These results suggest T1 ρ is not necessarily specific to underlying consolidation within the 30-min delay, but that those with longer T1 ρ in the right hemisphere also had performance deficits present at the end of the learning phase, and then, that performance deficit carried over to the delayed phase.

3.4.2. Some T1 ρ relationships strengthen after controlling for initial cognitive map formation

In a second follow-up analysis, to further understand the differences in relationships between hippocampal volume and T1 ρ with performance, we controlled for landmark location learning, which could affect how well participants perform in later tests. The residuals from landmark location learning as a predictor of other task outcomes (landmark location magnitude, delayed landmark location, and delayed wayfinding test) were added to the models testing relationships between T1 ρ and performance described above. For landmark location magnitude, a laterality interaction remained (laterality: $\beta = -0.32$, $t(246) = -2.37$, $p = .02$, subregion: $\beta = 0.04$, $t(246) = 0.33$, $p = .74$). In contrast, for delayed landmark location memory, the laterality interaction was no longer significant (laterality: $\beta = -0.25$, $t(246) = -1.88$, $p = .06$, subregion: $\beta = 0.11$, $t(246) = 0.78$, $p = .44$). Lastly, for delayed wayfinding test, bilateral T1 ρ remained a significant predictor after controlling for landmark location learning ($\beta = .20$, $t(80) = 2.73$, $p = .008$) with no interactions for subregion or laterality factors (subregion: $\beta = -.08$, $t(246) = -0.82$, $p = .41$, laterality: $\beta = .02$, $t(246) = 0.16$, $p = .87$). Overall, after controlling for initial cognitive map formation as assessed by landmark location learning, the relationships between T1 ρ and landmark location magnitude and delayed wayfinding test remained, while the relationship for delayed landmark location weakened, suggesting in part that the relationship between delayed landmark location and T1 ρ are regulated by initial cognitive map formation.

4. Discussion

The current study replicates and extends on previous research demonstrating a relationship between the hippocampus and spatial navigation in cognitively normal older adults. Regarding the cognitive relevance of the hippocampal anterior-posterior longitudinal axis, we did not find evidence for our predictions of the posterior hippocampus or right posterior hippocampus in either imaging measure, and we did not find support for the preferential role of the posterior hippocampus in retrieval during the delay phase. Overall, there are three important themes from our results. First, in cognitively normal older adults, T1 ρ and hippocampal volume have distinct individual differences that are related to different aspects of performance on this wayfinding task. Second, we found evidence for right lateralization in T1 ρ in relation to performance, but no regional specificity for relationships between hippocampal volume and performance outcomes. Third, delayed wayfinding test and landmark location memory are related to distinct imaging outcomes.

4.1. Main findings

Hippocampal volume and T1 ρ are related to different aspects of wayfinding performance. Hippocampal volume in this cross-sectional preclinical sample was more predictive of rapid-learning indexing cognitive map formation, whereas T1 ρ was more predictive of performance after initial learning and after a 30-minute delay. Right hippocampal volume generally predicts rapid learning of a cognitive map and our study partly replicates previous findings in a different task (Schinazi et al., 2013), albeit here bilateral hippocampal volume predicts cognitive map formation. However, hippocampal volume was not predictive of delayed wayfinding test performance as it was in Head & Isom (2010) and delayed wayfinding test did not show an anterior-posterior subregion or laterality interaction

as predicted from previous studies examining either plasticity (e.g., taxi drivers) or deterioration (e.g., Alzheimer's).

A few key differences exist between our study and Head & Isom (2010). In Head & Isom (2010), participants were given one 15-minute learning trial, followed by a shorter 10-minute delay. Here, participants were given four 5-minute learning trials, each followed by a 2-D map of the environment for object-location testing, shown to improve understanding of virtual layouts (Sjölander et al., 2005). Thus, in the task used here, participants had more total learning exposure and were given a 2-D framework to guide their cognitive map formation and internally resolve inconsistencies. Additionally, the start of a new learning trial allows a lost participant to restart or reorient themselves on a new learning trial, as opposed to freely wandering for 15 min in 1 trial. Thus, total time exposure, increased number of learning trials, 2-D map exposure for resolving inconsistencies, and increased delay time could all contribute to the lack of replication with Head & Isom (2010) for hippocampal volume with delayed wayfinding test. In addition to task differences, our older adult sample size was larger (84 vs 31), and both younger (63.6 ± 6.97 SD vs. 71 ± 8 SD) and more highly educated (16.8 ± 2.1 SD vs. 15.4 ± 3.1 SD), which may indicate age and education are moderators of the relationship between hippocampal volume and use of a cognitive map and should be examined in future studies with larger, more heterogeneous samples.

In our typical aging sample, we did find support for right lateralization for the relationship of longer T1 ρ with poorer cognitive map retrieval. The right lateralization in the T1 ρ models fits into previous findings of right lateralization in spatial navigation. While the data shown in Fig. 4F tend to show this relationship exists more so in the anterior than posterior, no 3-way interactions were statistically significant to support a further interaction with the anterior-posterior subregion factor. Surprisingly, there were no correlations between T1 ρ and hippocampal volume across hippocampal subregions. However, our followup analyses controlling for the association of hippocampal volume with cognitive map formation suggested some reordering of participants in performance from the end of the learning phase to the delayed condition, such that those with longer right hippocampal T1 ρ , but also larger hippocampal volume, performed better in the delay condition than participants with longer right hippocampal T1 ρ and smaller hippocampi. Participants with longer right hippocampal T1 ρ and smaller hippocampi were those most affected by the delay phase, which could be tested in a targeted fashion in follow-up studies. Overall, these results suggest that hippocampal T1 ρ is sensitive enough to detect spatial navigation differences in a healthy, preclinical sample, even independent from hippocampal volume. Given the evidence that MCI/AD pathology starts decades before diagnosis, and with T1 ρ 's detection capabilities in clinical samples, more longitudinal work with T1 ρ should be done to test its efficacy in predicting the development of MCI for use as an early detection tool.

Contrary to our hypothesis, we did not find evidence for lateralization or differences across the anterior-posterior longitudinal axis for hippocampal volume. This pattern of results for hippocampal volume is more in line with Weisberg et al. (2019) who found that there were no spatial navigation relationships among younger adults and hippocampal size, when considered either as total size, right hippocampus, or right posterior hippocampus. We did

not find regional specificity; however, our results suggest that in healthy aging populations, there are relationships with performance and total hippocampal size, even after controlling for age. This difference could present alternative explanations. First, in individuals with significant hippocampal atrophy, there are likely other aging processes occurring that could also influence performance, and hippocampal atrophy may be a proxy for a variety of co-occurring aging mechanisms impacting the broad spatial navigation network even when controlling for age. Future tests in young adults would need to be done with this task for direct comparability to Weisberg et al. (2019). A second possibility is that hippocampal size predicts spatial navigation performance in this spatial navigation test, but relationships may differ between hippocampal subregions and performance across other types of spatial navigation tests.

We see evidence for the second alternative within T1 ρ models, that different tests of spatial navigation memory representations are related to hippocampal health in distinct subregions. Longer bilateral T1 ρ was related to poorer delayed wayfinding test. However, within landmark location measures, it was related to right hippocampal T1 ρ only. One proposal is that the delayed wayfinding test condition benefits from constant position updating in real-time while traversing the maze to find object locations. Unfortunately, we did not do a goal-directed pointing task or test heading direction at the start of the 12 trials. Therefore, we did not get a measure of the accuracy of pre-trial cognitive map representation, and small undetected adjustments to goal-directed paths could be made throughout a given trial. Nonetheless, delayed wayfinding test is similar to the spatial navigation tests used in Iaria et al. (2007) and Maguire et al. (1998) which provide evidence for at least some functional support during navigation provided by the left hippocampus, which may in part explain the change of pattern from right lateralization to bilateral T1 ρ . On the other hand, landmark location was associated with right lateralized T1 ρ and the task is limited only to internal replay and requires translation of the internal cognitive map to a 2-D framework. This representation can only be updated from external cues between trials and not during trials like error adjustment in delayed wayfinding test.

4.2. Relation to preceding cerebrospinal fluid biomarker findings

This task has been used in several preceding papers, and the learning phase is largely comparable to Allison et al. (2016) and Allison et al. (2019) where participants were measured for CSF biomarkers of AD. In Allison et al. (2016), participants with positive CSF biomarker but cognitively normal profile showed poorer landmark location learning and performed similarly to the undiagnosed, early-phase symptomatic AD group. By the third trial, biomarker positive participants had recovered performance, but the symptomatic AD group had not. In the delay phase, both cognitively normal negative CSF biomarker and positive groups outperformed the symptomatic AD group. To relate this pattern to hippocampal measures in our study, we found variability in cognitive map formation was more strongly related to hippocampal volume, like the cognitively normal negative biomarker group. However, later measures of cognitive map usage were related to hippocampal T1 ρ , both at the end of the learning phase and the delayed phase, similar to the distinctly poorer performance of the symptomatic AD group of Allison et al. (2016). With this context, our results are consistent with the theory that hippocampal volume is

more sensitive to wayfinding deterioration in early preclinical phases and $T1\rho$ may be more sensitive to dysfunction associated with pathology. Altogether, our results suggest the combination of longer right hippocampal $T1\rho$ and spatial navigation performance deficits may be indicative of the potential for early MCI and/or a marker of advanced aging mechanisms. However, we note with caution that our results are from a cross-sectional design and it remains important to test the sensitivity of $T1\rho$ to age-related progression of pathology and cognitive decline in longitudinal designs.

4.3. Distinctions between hippocampal volume and $T1\rho$

Overall, it is unclear why the $T1\rho$ signal and hippocampal volume signals do not map onto each other in predicting performance, but we offer some proposals for reconciliation. In addition to individual differences in hippocampal volume, hippocampal volume is generally a broad indicator of brain health in aging, reflecting cumulating damage from years of atrophy and ultimately, leading to accelerating and predictable atrophy at a population level. $T1\rho$ is more of a heterogeneous signal than hippocampal volume, and even within an ROI's voxels there is a range of $T1\rho$ values that are associated with different pathology. On the lower end of a $T1\rho$ distribution, as Borthakur et al. (2006) showed, amyloid plaques in a mouse model can be seen on the $T1\rho$ image in comparison to histological slices, but this would only partially influence an ROI's median value. On the other hand, in clinical samples hippocampal and MTL $T1\rho$ values are elevated in MCI and AD (Borthakur et al., 2008; Haris et al., 2009, 2015; Haris et al., 2011). We believe elevated $T1\rho$ is setting the stage for future neurodegeneration via its association with pH and abnormal glucose metabolism. In past evaluation in phantoms (Magnotta et al., 2012; Owusu et al., 2020), $T1\rho$ increases when pH decreases. Additionally, a recent multi-modal neuroimaging paper has established $T1\rho$'s association with impaired glucose metabolism and amyloid burden across the cognitive spectrum, both of which are associated with tissue acidosis (Boles Ponto et al. 2020).

Based on Alzheimer's Disease Neuroimaging Initiative findings, structural changes (hippocampal volume) and changes in clinical function (memory tests) tend to occur closer in time than amyloid burden and tau-mediated neuronal injury and dysfunction (Weiner et al., 2017). With $T1\rho$'s relationship to amyloid burden, glucose metabolism, and acidity, we believe the $T1\rho$ curve would be most similar to the amyloid and tau curves, preceding structural changes in age-related pathology (Jack et al., 2013). Considering we have a cross-sectional sample of cognitively normal older adults, there would be greater lag between a subject's current trajectory and pathology-driven neurodegeneration and potential development of dementia, which would be consistent with a weak correlation between hippocampal $T1\rho$ and volume. Whereas in comparison to a subject with AD-related dementia, we would likely see convergence of longer $T1\rho$, smaller hippocampal volume, and poorer spatial navigation performance. Another reason $T1\rho$ signal may not map onto hippocampal volume is that it is measuring more transient protein aggregations and pathology burden based on $T1\rho$ signal's relation to abnormal glucose metabolism, which can reflect persistent abnormal function or transient reactivity to biological events.

4.4. Limitations

Our study has important findings that expand on a series of papers using the same task, but we acknowledge results should be interpreted with limitations that extend beyond the cross-sectional design. First, the landmark location learning task has not yet had a variant that has been used within the scanner to map functional activation during controlled implementation of cognitive map formation. However, other studies have performed similar tests to the delayed wayfinding test condition within the scanner (Hartley et al., 2003; Iaria et al., 2007; Maguire et al., 1998). Within our analyses, we acknowledge that the hippocampus is not the only area important for task performance and that a broad cortical network likely supports performance on this task as can be seen with most spatial navigation functional activation studies. Within our task, we do not have enough information regarding their wayfinding path and object sequence to profile different navigational and encoding strategies which may have an influence on the number of objects recalled. For example, a subject that follows the same path in each trial, encountering the objects in the same sequence, may perform differently than a subject that varies their path and object-sequences. Likewise, their specific path on a given trial would likely show some primacy and recency effects. With regards to demographics, another limitation is that our recruitment population tends to not be very diverse. Although our sample is mostly representative of the local population and typical of aging study recruitment, a high percentage of our subjects are highly educated, non-Hispanic white, and a higher percentage of females than males. Another limitation is in regard to the T1 ρ signal; in addition to metabolism, T1 ρ can be influenced by blood supply and saturation pulses and small velocity sensitizing gradients have been used to reduce the impact. Here, we note that these corrections were not used in this study, however, the value thresholding and taking median ROI values can help control for blood supply artifacts. This potential confound could be addressed in future studies together with measurement of hippocampal blood flow as an additional MR image modality. Lastly, we note to the reader to take some caution in interpretation; we did not correct for multiple comparisons for each of the 3 spatial navigation statistical tests and follow-up tests used in this study, and the effects described here would not survive a more stringent Bonferroni or FDR correction. We did, however, apply a domain-specific multiple comparisons correction, with a cut off of $p=.025$ to account for each imaging measure.

In future work, a comparison to younger and middle-aged adults with T1 ρ imaging would be beneficial to understand if lower T1 ρ across the lifespan is beneficial to performance or if T1 ρ is most useful for determining detrimental effects in advanced aging with elevated values.

5. Conclusion

In sum, our findings support that hippocampal volume and T1 ρ are measuring different aspects of hippocampal integrity among cognitively normal older adults and predict distinct outcomes of spatial navigation performance. These findings have implications for understanding the role of the hippocampus in age-related navigation decline and its impact on the hippocampal output to larger broad-based spatial navigation networks. This evidence

provides a link between younger adults and impaired groups and suggests the role of the hippocampus in spatial navigation is sensitive to healthy aging.

Supplementary Material

Refer to Web version on PubMed Central for supplementary material.

Acknowledgments

We thank the support from the Aging Mind and Brain Initiative at the University of Iowa (AMBI), National Institute of General Medical Sciences (NIGMS) (T32 GM108540), National Institute on Aging (NIA) (R01 AG055500), National Institute of Biomedical Imaging and Bioengineering (5R01EB022019), National Institute of Mental Health (5R01MH11578) and the MR imaging was performed on equipment supported by a high-end instrumentation grant (S10OD025025). Additionally, we thank Dr. Denise Head for providing the spatial navigation task, Conner Wharff for AMBI project management and data collection, Joel Bruss for work on in-house T1 ρ scripts, and the AMBI and Bike EXTEND study teams for their help with data collection.

Data availability

The code and data that support the findings of this study are available from the corresponding author upon reasonable request.

References

- Allison SL, Fagan AM, Morris JC, Head D, 2016. Spatial Navigation in Preclinical Alzheimer's Disease. *J. Alzheimer's Dis* 52, 77–90. doi:10.3233/JAD-150855. [PubMed: 26967209]
- Allison SL, Rodebaugh TL, Johnston C, Fagan AM, Morris JC, Head D, 2019. Developing a Spatial Navigation Screening Tool Sensitive to the Preclinical Alzheimer Disease Continuum. *Arch. Clin. Neuropsychol* 34, 1138–1155. doi:10.1093/arclin/acz019. [PubMed: 31197326]
- Bohbot VD, Lerch J, Thorndyraft B, Iaria G, Zijdenbos AP, 2007. Gray Matter Differences Correlate with Spontaneous Strategies in a Human Virtual Navigation Task. *J. Neurosci* 27, 10078–10083. doi:10.1523/JNEUROSCI.1763-07.2007. [PubMed: 17881514]
- Boles Ponto LL, Magnotta VA, Menda Y, Moser DJ, Oleson JJ, Harlynn EL, DeVries SD, Wemmie JA, Schultz SK, 2020. Comparison of T1Rho MRI, Glucose Metabolism, and Amyloid Burden Across the Cognitive Spectrum: A Pilot Study. *J. Neuropsychiatry Clin. Neurosci* 32, 352–361. doi:10.1176/appi.neuropsych.19100221. [PubMed: 32283991]
- Borthakur A, Gur T, Wheaton AJ, Corbo M, Trojanowski JQ, Lee VMY, Reddy R, 2006. In vivo measurement of plaque burden in a mouse model of Alzheimer's disease. *J. Magn. Reson. Imaging* 24, 1011–1017. doi:10.1002/jmri.20751. [PubMed: 17036339]
- Borthakur A, Sochor M, Davatzikos C, Trojanowski JQ, Clark CM, 2008. T1rho MRI of Alzheimer's disease. *Neuroimage* 41, 1199–1205. doi:10.1016/j.neuroimage.2008.03.030. [PubMed: 18479942]
- Burwell RD, 2004. Corticohippocampal Contributions to Spatial and Contextual Learning. *J. Neurosci* 24, 3826–3836. doi:10.1523/jneurosci.0410-04.2004. [PubMed: 15084664]
- Carr VA, Bernstein JD, Favila SE, Rutt BK, Kerchner GA, Wagner AD, 2017. Individual differences in associative memory among older adults explained by hippocampal subfield structure and function. *Proc. Natl. Acad. Sci. U. S. A* 114, 12075–12080. doi:10.1073/pnas.1713308114. [PubMed: 29078387]
- de Flores R, La Joie R, Landeau B, Perrotin A, Mézenge F, de La Sayette V, Eustache F, Desgranges B, Chételat G, 2015. Effects of age and Alzheimer's disease on hippocampal subfields. *Hum. Brain Mapp* 36, 463–474. doi:10.1002/hbm.22640. [PubMed: 25231681]
- Eichenbaum H, Cohen NJ, 2014. Can We Reconcile the Declarative Memory and Spatial Navigation Views on Hippocampal Function? *Neuron* 83, 764–770. doi:10.1016/j.neuron.2014.07.032. [PubMed: 25144874]

- Fjell AM, Westlye LT, Grydeland H, Amlie I, Espeseth T, Reinvang I, Raz N, Holland D, Dale AM, Walhovd KB, 2013. Critical ages in the life course of the adult brain: nonlinear subcortical aging. *Neurobiol. Aging* 34, 2239–2247. doi:10.1016/j.neurobiolaging.2013.04.006. [PubMed: 23643484]
- Foster CM, Kennedy KM, Hoagey DA, Rodrigue KM, 2019. The role of hippocampal subfield volume and fornix microstructure in episodic memory across the lifespan. *Hippocampus* 29, 1206–1223. doi:10.1002/hipo.23133. [PubMed: 31334583]
- Gorbach T, Pudas S, Lundquist A, Orädd G, Josefsson M, Salami A, de Luna X, Nyberg L, 2017. Longitudinal association between hippocampus atrophy and episodic-memory decline. *Neurobiol. Aging* 51, 167–176. doi:10.1016/j.neurobiolaging.2016.12.002. [PubMed: 28089351]
- Grady CL, Ryan JD, 2017, Age-Related Differences in the Human Hippocampus: Behavioral, Structural and Functional Measures BT - *The Hippocampus from Cells to Systems: Structure, Connectivity, and Functional Contributions to Memory and Flexible Cognition* In: Hannula DE, Duff MC (Eds.). Springer International Publishing, Cham, pp. 167–208. doi:10.1007/978-3-319-50406-3_7.
- Grön G, Wunderlich AP, Spitzer M, Tomczak R, Riepe MW, 2000. Brain activation during human navigation: gender-different neural networks as substrate of performance. *Nat. Neurosci* 3, 404–408. doi:10.1038/73980. [PubMed: 10725932]
- Haris M, McArdle E, Fenty M, Singh A, Davatzikos C, Trojanowski JQ, Melhem ER, Clark CM, Borthakur A, 2009. Early marker for Alzheimer's disease: hippocampus T1rho (T1ρ) estimation. *J. Magn. Reson. Imaging* 29, 1008–1012. doi:10.1002/jmri.21735. [PubMed: 19388096]
- Haris M, Singh A, Cai K, Davatzikos C, Trojanowski JQ, Melhem ER, Clark CM, Borthakur A, 2011a. T1rho (T1ρ) MR imaging in Alzheimer' disease and Parkinson's disease with and without dementia. *J. Neurol* 258, 380–385. doi:10.1007/s00415-010-5762-6. [PubMed: 20924593]
- Haris M, Singh A, Cai K, McArdle E, Fenty M, Davatzikos C, Trojanowski JQ, Melhem ER, Clark CM, Borthakur A, 2011b. T1ρ MRI in Alzheimer's Disease: Detection of Pathological Changes in Medial Temporal Lobe. *J. Neuroimaging* 21, e86–e90. doi:10.1111/j.1552-6569.2010.00467.x. [PubMed: 20331502]
- Haris M, Yadav SK, Rizwan A, Singh A, Cai K, Kaura D, Wang E, Davatzikos C, Trojanowski JQ, Melhem ER, Marincola FM, Borthakur A, 2015. T1rho MRI and CSF biomarkers in diagnosis of Alzheimer's disease. *NeuroImage Clin* 7, 598–604. doi:10.1016/j.nicl.2015.02.016. [PubMed: 25844314]
- Hartley T, Harlow R, 2012. An association between human hippocampal volume and topographical memory in healthy young adults. *Front. Hum. Neurosci* 6, 1–11. doi:10.3389/fnhum.2012.00338. [PubMed: 22279433]
- Hartley T, Maguire EA, Spiers HJ, Burgess N, 2003. The Well-Worn Route and the Path Less Traveled. *Neuron* 37, 877–888. doi:10.1016/S0896-6273(03)00095-3. [PubMed: 12628177]
- Head D, Isom M, 2010. Age effects on wayfinding and route learning skills. *Behav. Brain Res* 209, 49–58. doi:10.1016/j.bbr.2010.01.012. [PubMed: 20085784]
- Head D, Rodrigue KM, Kennedy KM, Raz N, 2008. Neuroanatomical and cognitive mediators of age-related differences in episodic memory. *Neuropsychology* 22 (4), 491–507. doi:10.1037/0894-4105.22.4.491. [PubMed: 18590361]
- Heo HY, Wemmie J, Thedens D, Magnotta VA, 2014. Evaluation of activity-dependent functional pH and T1ρ response in the visual cortex. *Neuroimage* 95, 336–343. doi:10.1016/j.neuroimage.2014.01.042. [PubMed: 24486980]
- Iaria G, Chen J-K, Guariglia C, Ptito A, Petrides M, 2007. Retrosplenial and hippocampal brain regions in human navigation: complementary functional contributions to the formation and use of cognitive maps. *Eur. J. Neurosci* 25, 890–899. doi:10.1111/j.1460-9568.2007.05371.x. [PubMed: 17298595]
- Iaria G, Petrides M, Dagher A, Pike B, Bohbot VD, 2003. Cognitive strategies dependent on the hippocampus and caudate nucleus in human navigation: variability and change with practice. *J. Neurosci* 23, 5945–5952 <https://doi.org/23/13/5945> [pii]. [PubMed: 12843299]
- Jack CR, Knopman DS, Jagust WJ, Petersen RC, Weiner MW, Aisen PS, Shaw LM, Vemuri P, Wiste HJ, Weigand SD, Lesnick TG, Pankratz VS, Donohue MC, Trojanowski JQ, 2013.

Tracking pathophysiological processes in Alzheimer's disease: an updated hypothetical model of dynamic biomarkers. *Lancet Neurol* 12, 207–216. doi:10.1016/S1474-4422(12)70291-0. [PubMed: 23332364]

- Johnson CP, Follmer RL, Oguz I, Warren LA, Christensen GE, Fiedorowicz JG, Magnotta VA, Wemmie JA, 2015a. Brain abnormalities in bipolar disorder detected by quantitative T1 ρ mapping. *Mol. Psychiatry* 20, 201–206. doi:10.1038/mp.2014.157. [PubMed: 25560762]
- Johnson CP, Thedens DR, Kruger SJ, Magnotta VA, 2020. Three-Dimensional GRE T 1 ρ mapping of the brain using tailored variable flip-angle scheduling. *Magn. Reson. Med* 84, 1235–1249. doi:10.1002/mrm.28198. [PubMed: 32052489]
- Johnson CP, Thedens DR, Magnotta VA, 2015b. Precision-guided sampling schedules for efficient T1 ρ mapping. *J. Magn. Reson. Imaging* 41, 242–250. doi:10.1002/jmri.24518. [PubMed: 24474423]
- Jung MW, Wiener SI, McNaughton BL, 1994. Comparison of spatial firing characteristics of units in dorsal and ventral hippocampus of the rat. *J. Neurosci* 14, 7347LP–737356. doi:10.1523/JNEUROSCI.14-12-07347.1994. [PubMed: 7996180]
- Kettunen MI, Gröhn OHJ, Silvennoinen MJ, Penttonen M, Kauppinen RA, 2002. Effects of intracellular pH, blood, and tissue oxygen tension on T1 ρ relaxation in rat brain. *Magn. Reson. Med* 48, 470–477. doi:10.1002/mrm.10233. [PubMed: 12210911]
- Konishi K, Bohbot VD, 2013. Spatial navigational strategies correlate with gray matter in the hippocampus of healthy older adults tested in a virtual maze. *Front. Aging Neurosci* 5, 1–8. doi:10.3389/fnagi.2013.00001. [PubMed: 23430962]
- Langnes E, Sneve MH, Sederevicius D, Amlien IK, Walhovd KB, Fjell AM, 2020. Anterior and posterior hippocampus macro- and microstructure across the lifespan in relation to memory—A longitudinal study. *Hippocampus* 30, 678–692. doi:10.1002/hipo.23189. [PubMed: 31961464]
- Lepage M, Habib R, Tulving E, 1998. Hippocampal PET activations of memory encoding and retrieval: the HIPER model. *Hippocampus* 8, 313–322. doi:10.1002/(SICI)1098-1063(1998)8:4<313::AID-HIPO1>3.0.CO;2-I. [PubMed: 9744418]
- Levine TF, Allison SL, Stojanovic M, Fagan AM, Morris JC, Head D, 2020. Spatial navigation ability predicts progression of dementia symptomatology. *Alzheimer's Dement* 16, 491–500. doi:10.1002/alz.12031. [PubMed: 32043719]
- Magnotta VA, Heo H-Y, Dlouhy BJ, Dahdaleh NS, Follmer RL, Thedens DR, Welsh MJ, Wemmie JA, 2012. Detecting activity-evoked pH changes in human brain. *Proc. Natl. Acad. Sci* 109, 8270–8273. doi:10.1073/pnas.1205902109, LP. [PubMed: 22566645]
- Maguire, Woollett, S., 2006. London Taxi Drivers and Bus Drivers. *Hippocampus* 1031, 1026–1031. doi:10.1002/hipo.
- Maguire EA, Burgess N, Donnett JG, Frackowiak RSJ, Frith CD, O'Keefe J, 1998. Knowing where and getting there: A human navigation network. *Science* 280, 921–924. doi:10.1126/science.280.5365.921, (80-). [PubMed: 9572740]
- Maguire EA, Gadian DG, Johnsrude IS, Good CD, Ashburner J, Frackowiak RSJ, Frith CD, 2000. Navigation-related structural change in the hippocampi of taxi drivers. *Proc. Natl. Acad. Sci. U. S. A* 97, 4398–4403. doi:10.1073/pnas.070039597. [PubMed: 10716738]
- Maguire EA, Nannery R, Spiers HJ, 2006. Navigation around London by a taxi driver with bilateral hippocampal lesions. *Brain* 129, 2894–2907. doi:10.1093/brain/awl286. [PubMed: 17071921]
- Meteyard L, Davies RAI, 2020. Best practice guidance for linear mixed-effects models in psychological science. *J. Mem. Lang* 112. doi:10.1016/j.jml.2020.104092.
- Moser EI, Kropff E, Moser M-B, 2008. Place Cells, Grid Cells, and the Brain's Spatial Representation System. *Annu. Rev. Neurosci* 31, 69–89. doi:10.1146/annurev.neuro.31.061307.090723. [PubMed: 18284371]
- Moser, Moser EI, 1999. Functional differentiation in the hippocampus. *Hippocampus* 8, 608–619. doi:10.1002/(SICI)1098-1063(1998)8:6<608::AID-HIPO3>3.0.CO;2-7.
- Nedelska Z, Andel R, Laczó J, Vlcek K, Horinek D, Lisy J, Sheardova K, Bureš J, Hort J, 2012. Spatial navigation impairment is proportional to right hippocampal volume. *Proc. Natl. Acad. Sci. U. S. A* 109, 2590–2594. doi:10.1073/pnas.1121588109. [PubMed: 22308496]

- Nestrasil I, Michaeli S, Liimatainen T, Rydeen CE, Kotz CM, Nixon JP, Hanson T, Tuite PJ, 2010. T1rho and T2rho MRI in the evaluation of Parkinson's disease. *J. Neurol* 257, 964–968. doi:10.1007/s00415-009-5446-2. [PubMed: 20058018]
- Owusu N, Johnson CP, Kearney W, Thedens D, Wemmie J, Magnotta VA, 2020. R1 ρ sensitivity to pH and other compounds at clinically accessible spin-lock fields in the presence of proteins. *NMR Biomed* 33, e4217. doi:10.1002/nbm.4217. [PubMed: 31742802]
- Poppenk J, Evensmoen HR, Moscovitch M, Nadel L, 2013. Long-axis specialization of the human hippocampus. *Trends Cogn. Sci* 17, 230–240. doi:10.1016/j.tics.2013.03.005. [PubMed: 23597720]
- Poppenk J, Moscovitch M, 2011. A hippocampal marker of recollection memory ability among healthy young adults: Contributions of posterior and anterior segments. *Neuron* 72, 931–937. doi:10.1016/j.neuron.2011.10.014. [PubMed: 22196329]
- Raz N, Lindenberger U, Rodrigue KM, Kennedy KM, Head D, Williamson A, Dahle C, Gerstorf D, Acker JD, 2005. Regional brain changes in aging healthy adults: general trends, individual differences and modifiers. *Cereb. Cortex* 15, 1676–1689. doi:10.1093/cercor/bhi044. [PubMed: 15703252]
- Redfield AG, 1955. Nuclear magnetic resonance saturation and rotary saturation in solids. *Phys. Rev* 98, 1787–1809. doi:10.1103/PhysRev.98.1787.
- Schinazi VR, Nardi D, Newcombe NS, Shipley TF, Epstein RA, 2013. Hippocampal size predicts rapid learning of a cognitive map in humans. *Hippocampus* 23, 515–528. doi:10.1002/hipo.22111. [PubMed: 23505031]
- Sepponen RE, Pohjonen JA, Sipponen JT, Tanttu JI, 1985. A Method for T1 ρ Imaging. *J. Comput. Assist. Tomogr* doi:10.1097/00004728-198511000-00002.
- Sherrill KR, Erdem UM, Ross RS, Brown TI, Hasselmo ME, Stern CE, 2013. Hippocampus and retrosplenial cortex combine path integration signals for successful navigation. *J. Neurosci* 33, 19304–19313. doi:10.1523/JNEUROSCI.1825-13.2013. [PubMed: 24305826]
- Sjölander M, Höök K, Nilsson LG, Andersson G, 2005. Age differences and the acquisition of spatial knowledge in a three-dimensional environment: evaluating the use of an overview map as a navigation aid. *Int. J. Hum. Comput. Stud* 63, 537–564. doi:10.1016/j.ijhcs.2005.04.024.
- Smith M.Lou, Milner B, 1981. The role of the right hippocampus in the recall of spatial location. *Neuropsychologia* 19, 781–793. doi:10.1016/0028-3932(81)90090-7. [PubMed: 7329524]
- Spaniol J, Davidson PSR, Kim ASN, Han H, Moscovitch M, Grady CL, 2009. Event-related fMRI studies of episodic encoding and retrieval: Meta-analyses using activation likelihood estimation. *Neuropsychologia* 47, 1765–1779. doi:10.1016/j.neuropsychologia.2009.02.028. [PubMed: 19428409]
- Tolman EC, 1948. Cognitive maps in rats and men. *Psychol. Rev* doi:10.1037/h0061626.
- Wáng Y-XJ, Zhang Q, Li X, Chen W, Ahuja A, Yuan J, 2015. T1 ρ magnetic resonance: basic physics principles and applications in knee and intervertebral disc imaging. *Quant. Imaging Med. Surg* 5, 858–885. doi:10.3978/j.issn.2223-4292.2015.12.06. [PubMed: 26807369]
- Wassef SN, Wemmie J, Johnson CP, Johnson H, Paulsen JS, Long JD, Magnotta VA, 2015. T1 ρ imaging in premanifest Huntington disease reveals changes associated with disease progression. *Mov. Disord* 30, 1107–1114. doi:10.1002/mds.26203. [PubMed: 25820773]
- Wegman J, Fonteijn HM, van Ekert J, Tyborowska A, Jansen C, Janzen G, 2014. Gray and white matter correlates of navigational ability in humans. *Hum. Brain Mapp* 35, 2561–2572. doi:10.1002/hbm.22349. [PubMed: 24038667]
- Weiner MW, Veitch DP, Aisen PS, Beckett LA, Cairns NJ, Green RC, Harvey D, Jack CR, Jagust W, Morris JC, Petersen RC, Saykin AJ, Shaw LM, Toga AW, Trojanowski JQ, 2017. Recent publications from the Alzheimer's Disease Neuroimaging Initiative: reviewing progress toward improved AD clinical trials. *Alzheimer's Dement* 13, e1–e85. doi:10.1016/j.jalz.2016.11.007. [PubMed: 28342697]
- Weisberg SM, Newcombe NS, Chatterjee A, 2019. Everyday taxi drivers: do better navigators have larger hippocampi? *Cortex* 115, 280–293. doi:10.1016/j.cortex.2018.12.024. [PubMed: 30884282]

- Wolbers T, Büchel C, 2005. Dissociable retrosplenial and hippocampal contributions to successful formation of survey representations. *J. Neurosci* 25, 3333–3340. doi:10.1523/JNEUROSCI.4705-04.2005. [PubMed: 15800188]
- Wollett K, Maguire EA, 2011. Acquiring “the knowledge” of London’s layout drives structural brain changes. *Curr. Biol* 21, 2109–2114. doi:10.1016/j.cub.2011.11.018. [PubMed: 22169537]

Author Manuscript

Author Manuscript

Author Manuscript

Author Manuscript

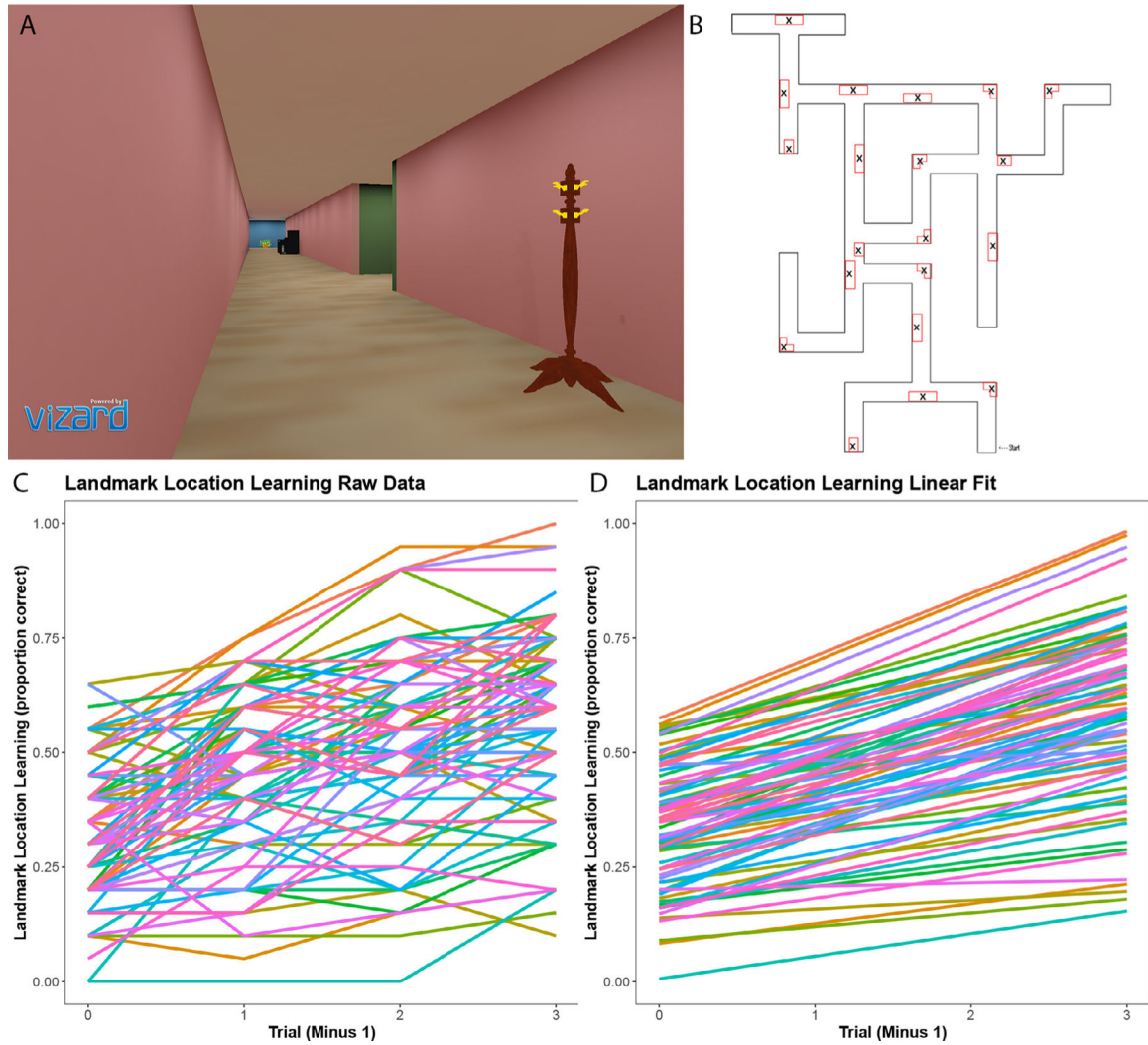


Fig. 1. Wayfinding Navigation Task and Behavioral Performance.

A) Subjects traverse a virtual maze with a joystick while instructed to pay attention to object locations. B) Subjects are asked to mark X's where object locations are in a maze shown as a 2-dimensional representation. C) # of objects correct out of 20 for each subject is scored across 4 trials. Trial is represented as trial minus 1 for interpretation of statistical intercept. D) Linear model fit for each subject, model intercept is used in subsequent analyses.

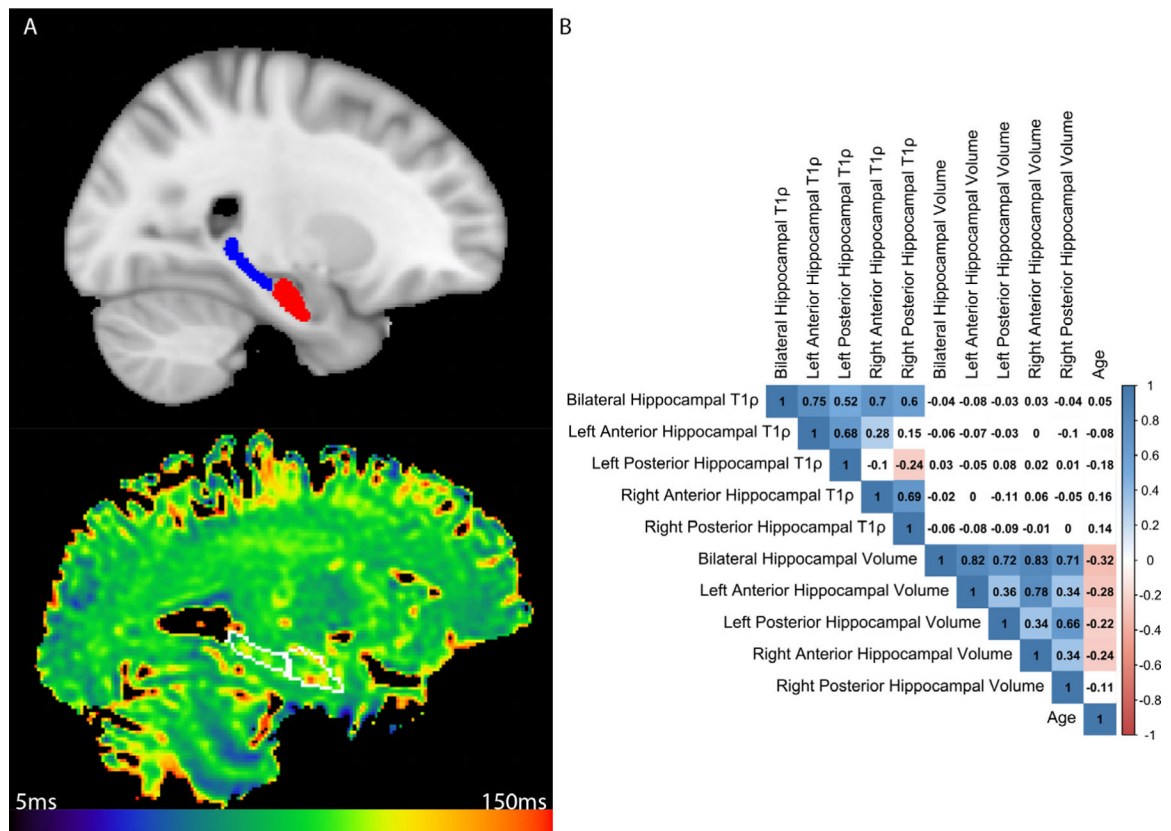


Fig. 2. Hippocampal Volume and T1 ρ Segmentations and Correlations.

A) Hippocampal mask in MNI space. Anterior-posterior subregion segmentation at $y=-21$ (red = anterior, blue = posterior) and then transformed back to each subject space for volume and median T1 ρ values. Bottom image, whole brain T1 ρ map with white hippocampal mask outline. Heterogeneity within ROI can be seen in anterior hippocampus. T1 ρ map is filtered to values between 5 and 150 ms to further eliminate cerebrospinal fluid bias. B) Correlation map of hippocampal segmentations and age.. Age is coded in chronological years. Correlations with p 's < 0.05 are highlighted with corresponding positive color (blue) or negative color (red).

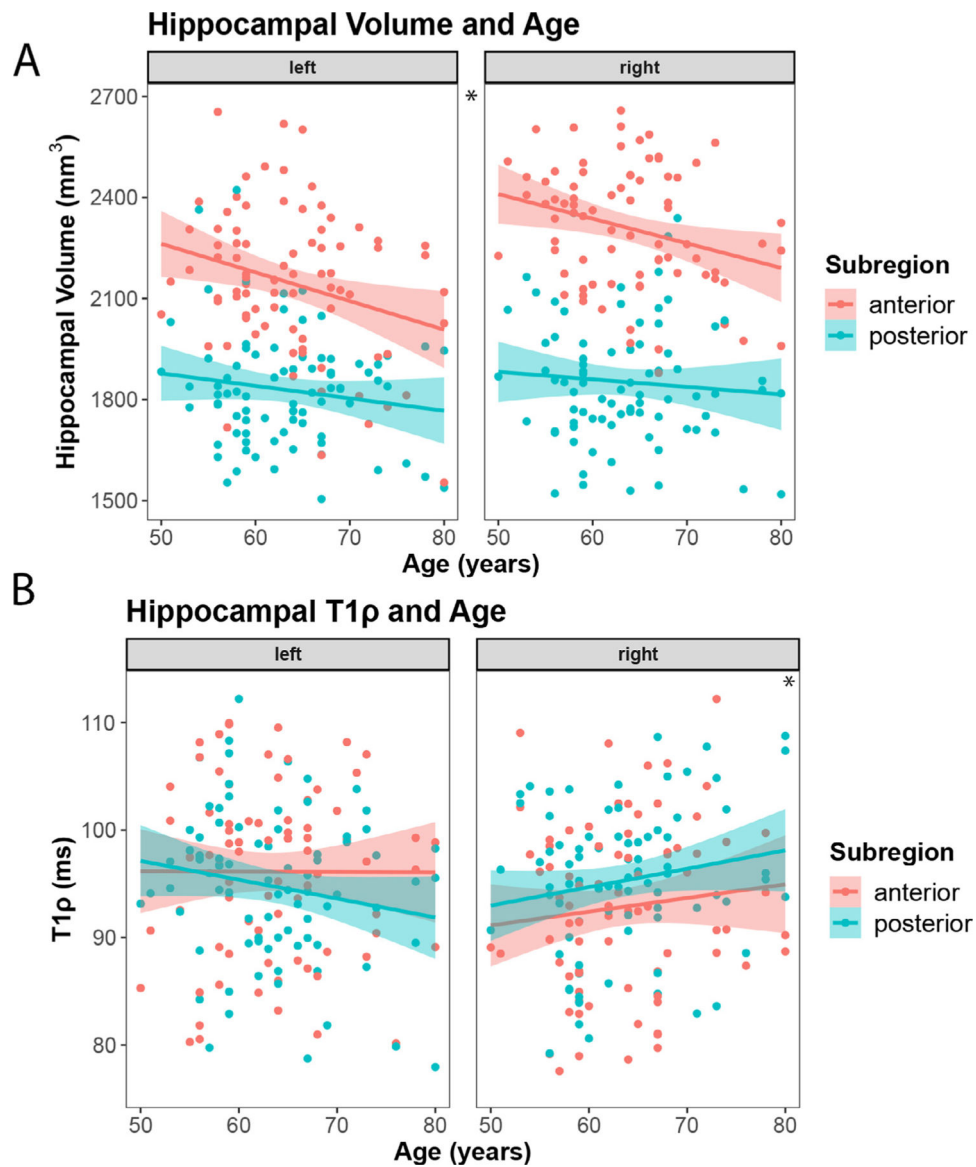


Fig. 3. Hippocampal Volume and T1 ρ Relationships with Age.

Each graph is paneled to show left and right hippocampus. Anterior-posterior subregion is noted by color (red = anterior, blue = posterior). A) Age is predictive of smaller hippocampal volume (mm^3) across all segmentations. B) Age is predictive of longer T1 ρ (ms) only in the right hippocampus. * $p < .025$.

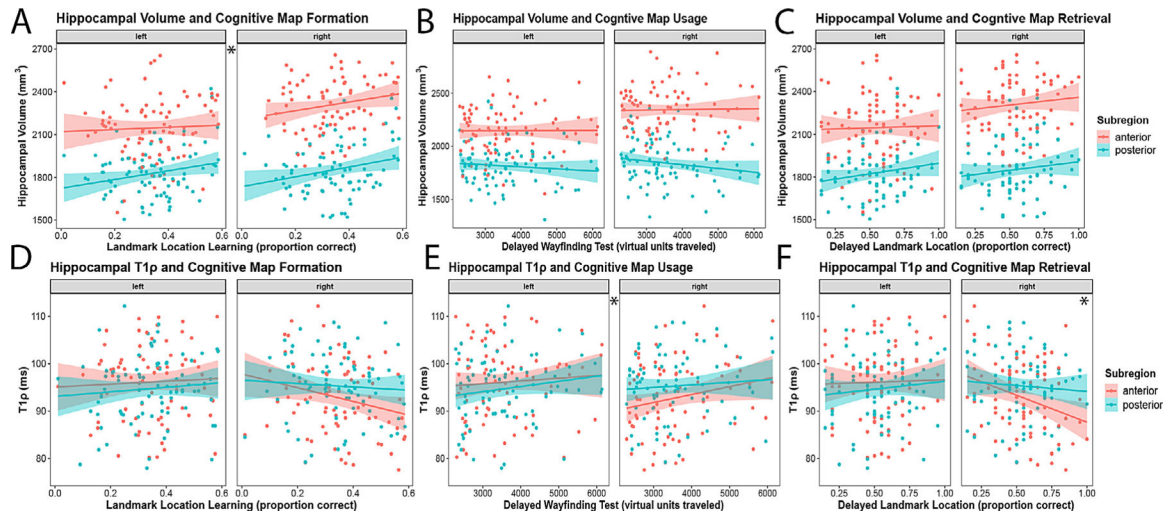


Fig. 4. Hippocampal Volume and T1 ρ Relationships with Spatial Navigation Outcomes.

All models contain factors of anterior-posterior subregion and laterality for different hippocampal segmentations and control for age and sex. Each graph is paneled to show left and right hippocampus. Anterior-posterior subregion is noted by color (red = anterior, blue = posterior). Imaging measures are presented on the y-axis to match statistical models which include interactions of subregion and laterality with cognitive variables of interest. A) Larger hippocampal volume (mm^3) is related to better cognitive map formation as measured by landmark location learning (proportion correct). B) Hippocampal volume is not related to cognitive map usage as measured by average virtual units traveled across 12 trials in delayed wayfinding test. C) Hippocampal volume is not related to cognitive map retrieval as measured by delayed landmark location (proportion correct). D) T1 ρ (relaxation rate in ms) is not related to cognitive map formation. E) Longer T1 ρ is generally related to poorer cognitive map usage. F) Longer right hippocampal T1 ρ is related to poorer cognitive map retrieval. * $p < .025$.

There were no significant differences between parent study 1 and parent study 2 for age ($t(82) = 0.68, p = .5$), sex ($t(82) = 0, p = 1$), or years of education ($t(82) = 1.69, p = .1$).

Table 1

Demographics				
Parent Study:	1	2	Pooled Sample	Min-Max
Subjects	36	48	84	
% Female	58.33	58.33	58.33	
Age (Mean \pm SD)	64.19 \pm 7.6	63.15 \pm 6.51	63.6 \pm 6.97	50–80
Years of Education (Mean \pm SD)	17.39 \pm 3.05	16.35 \pm 2.56	16.8 \pm 2.81	12–25

Table 2

Sample mean and SD values for hippocampal segmentations and cognitive outcomes. Sample mean T1 ρ (ms) is calculated from subject specific median voxel T1 ρ values (ms). Volume estimates (mm³) for each hippocampal segmentation are adjusted for intracranial volume. Landmark Location Learning, Magnitude, and Delayed Landmark Location are proportion correct out of 20 objects. Delayed Wayfinding test is the average virtual units traveled across 12 trials.

Descriptive Statistics		
	Mean \pm SD	Min-Max
Left Anterior Hipp T1 ρ (ms)	93.91 \pm 10.71	65.00–115.85
Left Posterior Hipp T1 ρ (ms)	94.20 \pm 8.06	77.96–114.35
Right Anterior Hipp T1 ρ (ms)	90.24 \pm 10.42	62.98–115.36
Right Posterior Hipp T1 ρ (ms)	92.932 \pm 8.39	73.26–108.76
Left Anterior Hipp Vol. (mm ³)	2146.88 \pm 214.52	1553.68–2654.41
Left Posterior Hipp Vol. (mm ³)	1813.99 \pm 184.54	1308.56–2422.12
Right Anterior Hipp Vol. (mm ³)	2343.61 \pm 216.95	1879.05–2890.02
Right Posterior Hipp Vol. (mm ³)	1840.59 \pm 197.48	1333.91–2353.48
Landmark Location Learning (proportion correct)	0.34 \pm 0.13	.01–0.59
Landmark Location Magnitude (proportion correct)	0.58 \pm 0.20	.10–1.00
Delayed Wayfinding Test (virtual units)	3512.89 \pm 897.97	2288.18–6004.21
Delayed Landmark Location (proportion correct)	0.54 \pm 0.20	.15–1.00

Table 3

All linear mixed models include age and sex as covariates. Age measured as chronological age in years; sex coded as $M=0$, $F=1$; laterality coded as $L=-0.5$, $R=0.5$, subregion coded as anterior= -0.5 , posterior= 0.5 . All beta coefficients reflect standardized regression weights. The above table shows linear mixed models with respect to spatial navigation outcomes (learning: landmark location intercept, test: delayed wayfinding test, and delayed: delayed landmark location) and Hippocampal T1 ρ (relaxation time in ms) and volume (mm³).

Linear Mixed Models		
Predictors	Hippocampal T1 ρ	Hippocampal Volume
(Intercept)	-0.22	0.01
Age	0.07	-0.22*
Sex	0.37*	-0.01
Age:Laterality	0.28**	0.07
Age:Subregion	-0.06	0.09
Age:Laterality:Subregion	0.08	0.08
R ²	0.27	0.48
(Intercept)	-0.23*	0.04
Age	0.07	-0.22*
Sex	0.39*	-0.07
Learning	-0.05	0.19*
Learning:Laterality	-0.17	0.07
Learning:Subregion	0.08	0.14
Learning:Laterality:Subregion	0.22	-0.13
R ²	0.27	0.49
(Intercept)	-0.25*	0.01
Age	0.03	-0.21*
Sex	0.42**	-0.01
Test	0.20*	0.00
Test:Laterality	0.06	-0.01
Test:Subregion	-0.10	-0.15
Test:Laterality:Subregion	-0.19	-0.09
R ²	0.26	0.49
(Intercept)	-0.22	0.01
Age	0.07	-0.20*
Sex	0.37*	-0.01
Delayed	-0.03	0.09
Delayed:Laterality	-0.23*	0.04
Delayed:Subregion	0.12	0.12
Delayed:Laterality:Subregion	0.25	-0.09
R ²	0.28	0.48

**
 $p < .01$;

*
 $p < .025$.

Author Manuscript

Author Manuscript

Author Manuscript

Author Manuscript